nature chemical biology

Coupling ligand structure to specific conformational switches in the β_2-adrenoceptor

Xiaojie Yao[1,3], Charles Parnot[1,3], Xavier Deupi[1], Venkata R P Ratnala[1], Gayathri Swaminath[1], David Farrens[2] & Brian Kobilka[1]

G protein–coupled receptors (GPCRs) regulate a wide variety of physiological functions in response to structurally diverse ligands ranging from cations and small organic molecules to peptides and glycoproteins. For many GPCRs, structurally related ligands can have diverse efficacy profiles. To investigate the process of ligand binding and activation, we used fluorescence spectroscopy to study the ability of ligands having different efficacies to induce a specific conformational change in the human β_2-adrenoceptor (β_2-AR). The 'ionic lock' is a molecular switch found in rhodopsin-family GPCRs that has been proposed to link the cytoplasmic ends of transmembrane domains 3 and 6 in the inactive state[1–3]. We found that most partial agonists were as effective as full agonists in disrupting the ionic lock. Our results show that disruption of this important molecular switch is necessary, but not sufficient, for full activation of the β_2-AR.

The $Asp^{3.49}$-$Arg^{3.50}$ pair (numbering according to the Ballesteros general scheme; see Methods) at the cytoplasmic end of transmembrane domain 3 (TM3) is part of the highly conserved (D/E)RY motif found in β_2-AR and other rhodopsin-family GPCRs, whereas the $Glu^{6.30}$ at the cytoplasmic end of TM6 is highly conserved in amine and opsin receptors. The ionic link between the $Asp^{3.49}$-$Arg^{3.50}$ pair and $Glu^{6.30}$ (also known as the ionic lock, **Fig. 1**) has been proposed to maintain GPCRs in the resting state[1–3] and was shown to be disrupted after photoactivation of rhodopsin[4]. Thus, disruption of the ionic lock represents a molecular switch that may be required for the activation of rhodopsin-family GPCRs. Previous biophysical studies on the β_2-AR suggest that agonist binding and activation occurs through at least one conformational intermediate, implying that more than one molecular switch is involved[5–7]. These studies also show that structurally different agonists and partial agonists differ in their ability to induce specific conformational transitions.

To study the effect of different classes of ligands on the ionic lock of β_2-AR, we generated a modified receptor having a fluorescence reporter that monitors movement between the cytoplasmic ends of TM3 and TM6. According to a three-dimensional model of the β_2-AR (**Fig. 1**), $Ala271^{6.33}$ and $Ile135^{3.54}$ are close to each other (Cα-Cα distance ~11 Å) yet separated by the ionic lock. These residues are well positioned for using the bimane-tryptophan technique, which relies on the quenching of bimane fluorescence by tryptophan at near-contact distances in the 5- to 15-Å range[8]. We mutated $Ala271^{6.33}$ to cysteine on a minimal-cysteine β_2-AR background (**Fig. 1a**) to generate β_2-AR–Δ5-Cys271. $Cys271^{6.33}$ in β_2-AR–Δ5-Cys271 was more reactive than any of the remaining cysteines in β_2-AR–Δ5-Cys271 (**Supplementary Fig. 1** online) and could be specifically labeled with monobromobimane (mBBr, **1**). We also mutated $Ile135^{3.54}$ to tryptophan to generate β_2-AR–Δ5-Cys271+Trp135. Our β_2-AR model predicts that in the absence of ligand, the ionic lock keeps TM6 in a distorted conformation, markedly decreasing the helical twist at the level of the highly conserved proline kink at $Pro288^{6.50}$. The bimane on $Cys271^{6.33}$ is then restricted by the ionic lock and lies in a pocket formed by residues in TM2, TM6 and TM7. The quencher $Trp135^{3.54}$ is located one turn below $Arg131^{3.50}$. Thus, the ionic lock separates the fluorophore and the quencher, and no direct contact between the two is possible (**Fig. 1c,d**). When the ionic lock breaks upon receptor activation, TM6 is released and moves away from TM3. This rearrangement opens a crevice in the cytoplasmic region of the receptor. The fluorophore on $Cys271^{6.33}$ is no longer restricted by the ionic lock and can approach $Trp135^{3.54}$, which should result in decreased fluorescence intensity (**Fig. 1c,d**). This prediction is also consistent with a previous study of the homologous residues in rhodopsin using spin probes[4].

The modified receptors β_2-AR–Δ5-Cys271 and β_2-AR–Δ5-Cys271+Trp135 had ligand-binding affinities (**Supplementary Table 1** online) that are not notably different from those previously reported for wild-type β_2-AR (ref. 9). Moreover, labeling of Cys271 with bimane did not substantially alter agonist-binding affinity (**Supplementary Fig. 2** online). We measured the fluorescence properties of bimane bound to $Cys271^{6.33}$ in the presence and absence of $Trp135^{3.54}$ by comparing bimane-labeled β_2-AR–Δ5-Cys271 with bimane-labeled β_2-AR–Δ5-Cys271+Trp135. The bimane spectra for both constructs showed maximal emission at 460 nm and were very similar in shape, having nearly the same emission peak (**Fig. 2a,b**). Thus, the tryptophan introduced at position $135^{3.54}$ did not substantially perturb the microenvironment of the bimane label at $Cys271^{6.33}$. After

[1]Department of Molecular and Cellular Physiology, Stanford University School of Medicine, 279 Campus Drive, Stanford, Palo Alto, California 94305, USA. [2]Departments of Biochemistry and Molecular Biology, Oregon Health & Science University, 3181 Southwest Sam Jackson Park Drive, Portland, Oregon 97201-3098, USA. [3]These authors contributed equally to this work. Correspondence should be addressed to B.K. (kobilka@stanford.edu).

Received 20 December 2005; accepted 16 May 2006; published online 25 June 2006; doi:10.1038/nchembio801

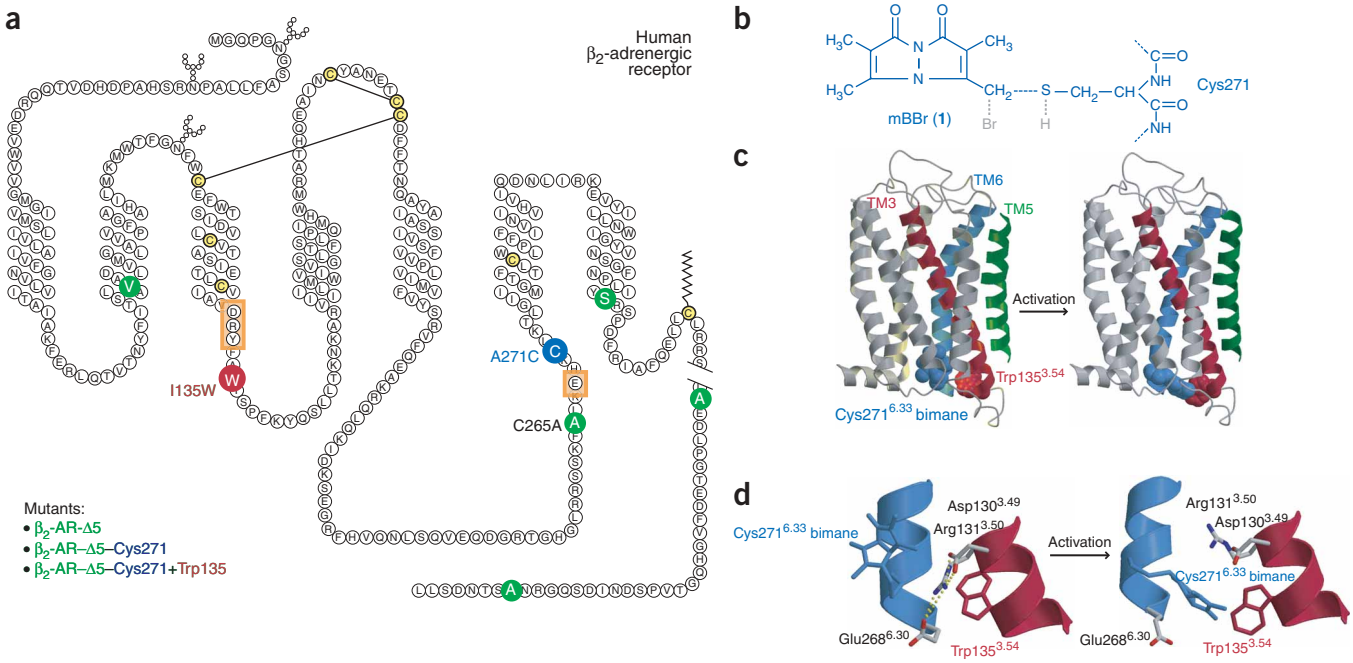

Figure 1 Molecular model of the β_2-AR. (**a**) Mutations I135W and A271C introduced for the bimane assay are shown in red and blue, respectively. The mutations introduced to remove endogenous cysteines are shown in green. The unreactive remaining cysteines are shown in yellow. The conserved positions involved in the ionic lock structure are outlined in orange. (**b**) Labeling of C271 with mBBr, showing the short linker introduced by the reaction. (**c**) Molecular model of the β_2-AR. The position of β_2-AR residues are followed by the Ballesteros general number[18] in superscript, in the form X.YY, in which X refers to the TM segment and YY to the position relative to the most highly conserved amino acid in the TM segment, which is assigned an arbitrary position of 50. Bimane-labeled Cys271$^{6.33}$ and Trp135$^{3.54}$ are shown as solid spheres. In the inactive state, bimane is fluorescent (left). On activation, the movement of TM6 allows the rearrangement of the bimane and Trp135$^{3.54}$ side chains, resulting in bimane quenching and a decrease in fluorescence (right). (**d**) Detail of the environment of bimane. In the inactive state the ionic lock (yellow dots) between TM3 and TM6 (Asp130$^{3.49}$, Arg131$^{3.50}$ and Glu268$^{6.30}$) prevents direct contact between bimane and Trp135$^{3.54}$ (left). On activation, the ionic lock is broken and bimane can approach Trp135$^{3.54}$ (right).

normalizing for receptor concentration, we found the brightness of the bimane to be only marginally smaller for β_2-AR–Δ5-Cys271+Trp135 than for β_2-AR–Δ5-Cys271, which showed that there is no substantial quenching of bimane-Cys271$^{6.33}$ by Trp135$^{3.54}$ in the inactive state of β_2-AR, as predicted by our model.

We next determined the effects of ligands with different structures and efficacies on bimane fluorescence intensity. We observed a 48%, 47% and 46% decrease in bimane intensity for the full agonists isoproterenol (**2**) and epinephrine (**3**) and the noncatechol partial agonist salbutamol (**4**), respectively (**Fig. 2c,d**). The antagonist alprenolol (**5**) and the inverse agonist ICI-118,551 (**6**) had very little effect on the bimane fluorescence intensity. The responses to agonists were specifically due to tryptophan quenching, as we obtained only small upward responses in the control construct β_2-AR–Δ5-Cys271, in which Trp135$^{3.54}$ is absent (**Fig. 2c**). There was no substantial change in the wavelength of the emission peak after agonist treatment (**Fig. 2b**), suggesting a quenching interaction with no change in polarity around the bimane fluorophore.

The conformational transition detected by the quenching of bimane fluorescence (that is, the disruption of the ionic lock between TM3 and TM6; **Fig. 1c,d**) is therefore specific for agonists. To discover the structural determinants of agonists that are responsible for this specific conformational change, we measured the fluorescence response to a set of catechol and noncatechol agonists having different affinities and efficacies, ranging from full agonists to weak partial agonists. We determined the dose response for the catecholamine agonists isoproterenol, epinephrine, norepinephrine (**7**) and dopamine (**8**), as well as for the noncatecholamine partial agonists salbutamol and halostachine (**9**), and for catechol (**10**; **Fig. 3**). All catecholamine agonists gave the same maximal response in the bimane assay. This result was notable because dopamine is a weak partial agonist for the wild-type, unlabeled receptor. To confirm that dopamine is also a partial agonist for the bimane-labeled β_2-AR–Δ5-Cys271+Trp135, we reconstituted the purified, labeled receptor with stimulatory G protein for adenylyl cyclase (G_s) and measured agonist-stimulated [γ-^{35}S]GTP binding. It should be noted that G protein activation by β_2-AR–Δ5-Cys271+Trp135 is impaired relative to wild-type β_2-AR, most likely owing to a steric effect of the Trp135 mutation; nevertheless, we were able to detect a significant difference in [γ-^{35}S]GTP binding stimulated by dopamine and isoproterenol ($P < 0.01$; **Fig. 4a**). Thus, dopamine is as efficacious as isoproterenol at disrupting the ionic lock, yet this conformational change is not sufficient to induce full activation of the receptor.

Noncatechol partial agonists also triggered changes in bimane fluorescence, with salbutamol inducing 95% of the response observed for isoproterenol (whereas halostachine, a very weak partial agonist, induced 50% of the response seen for isoproterenol). For all of these ligands, the effector concentration for half-maximum response (EC_{50}) in the bimane assay was consistent with the affinity measured in competition binding assay (**Fig. 3b**).

Catechol was the only partial agonist that produced no quenching of bimane fluorescence. We previously showed that catechol (i) induces a conformational response in β_2-AR labeled with tetramethylrhodamine on Cys265$^{6.27}$ and (ii) is a weak partial agonist in a

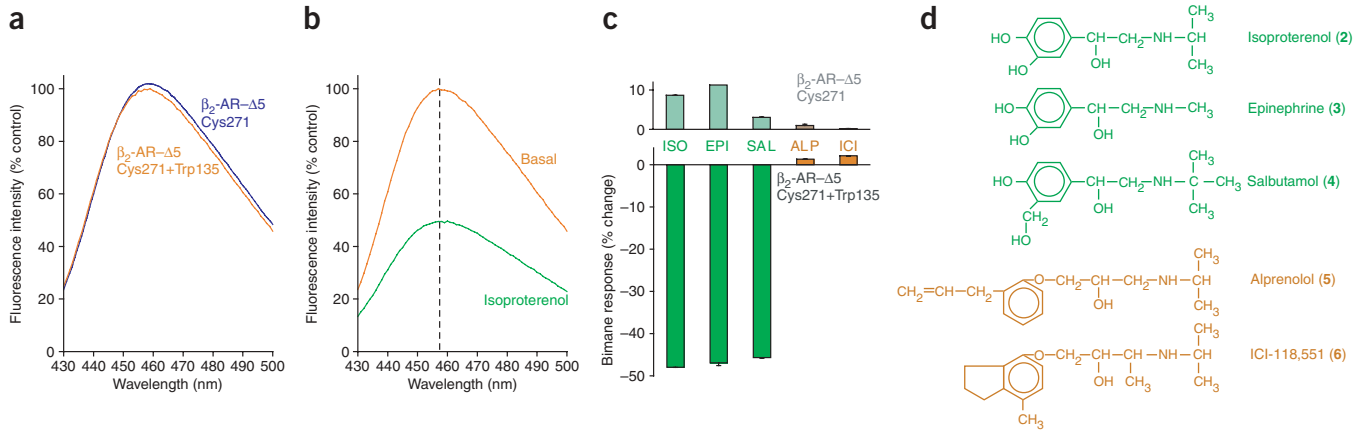

Figure 2 Fluorescence intensity of the bimane-attached Cys271. (**a**) Fluorescence emission spectra of the purified bimane-labeled receptors β_2-AR–Δ5-Cys271 (blue line) and β_2-AR–Δ5-Cys271+Trp135 (orange line) in detergent micelles. The excitation wavelength was 390 nm. The signal was corrected by dividing the fluorescence signal by the receptor concentration and normalizing to 100% for the construct β_2-AR–Δ5-Cys271+Trp135. The amount of receptor used for measurements was typically around 10 fmol. (**b**) Emission scans of bimane fluorescence before (orange) and after (green) stimulation with the full agonist isoproterenol. The intensity was normalized to 100% for the maximal intensity in the basal condition. The emission scan shows a strong reduction in fluorescence intensity but no change in the wavelength of maximal emission. (**c**) Maximal bimane responses to the full agonists isoproterenol and epinephrine, the partial agonist salbutamol, the neutral antagonist alprenolol and the inverse agonist ICI-118,551. The bimane response was measured as the percentage of fluorescence intensity change over the basal signal, as measured in the absence of any ligands. The top bars show the responses for the control β_2-AR–Δ5-Cys271. The bottom bars show the responses for β_2-AR–Δ5-Cys271+Trp135. Data are presented as the mean ± s.e.m. from three to seven independent experiments. (**d**) Chemical structure of the ligands used for the experiment in **c**. Isoproterenol and epinephrine are catecholamine agonists, salbutamol is a noncatechol partial agonist, alprenolol is an antagonist and ICI-118,551 is an inverse agonist.

[γ-^{35}S]GTP binding assay on wild-type β_2-AR[7]. We also found that catechol competes for binding with catecholamines but not with noncatechol partial agonists or antagonists. We proposed that catechol occupies the same binding site as the catechol ring in catecholamines and is thereby able to activate another molecular switch, a rotamer toggle switch in TM6 that has been suggested to be involved in the activation of amine and opsin receptor families[10]. On binding, the aromatic catechol ring of catecholamines presumably has a direct interaction with the aromatic residues of the rotamer toggle switch, Trp286$^{6.48}$ and Phe290$^{6.52}$. Monte Carlo simulations suggest that rotamer configurations of Cys285$^{6.47}$, Trp286$^{6.48}$ and Phe290$^{6.52}$, the residues that comprise the rotamer toggle switch, are coupled and modulate the bend angle of TM6 around the highly conserved proline kink at Pro288$^{6.50}$, leading to the movement of the cytoplasmic end of TM6 on activation[10]. We found that a saturating concentration of catechol had no effect on the ionic lock (**Fig. 3a**), even though we could detect catechol binding to bimane-labeled β_2-AR–Δ5-Cys271+Trp135 in a modified competition assay (**Fig. 4b,c**). Thus,

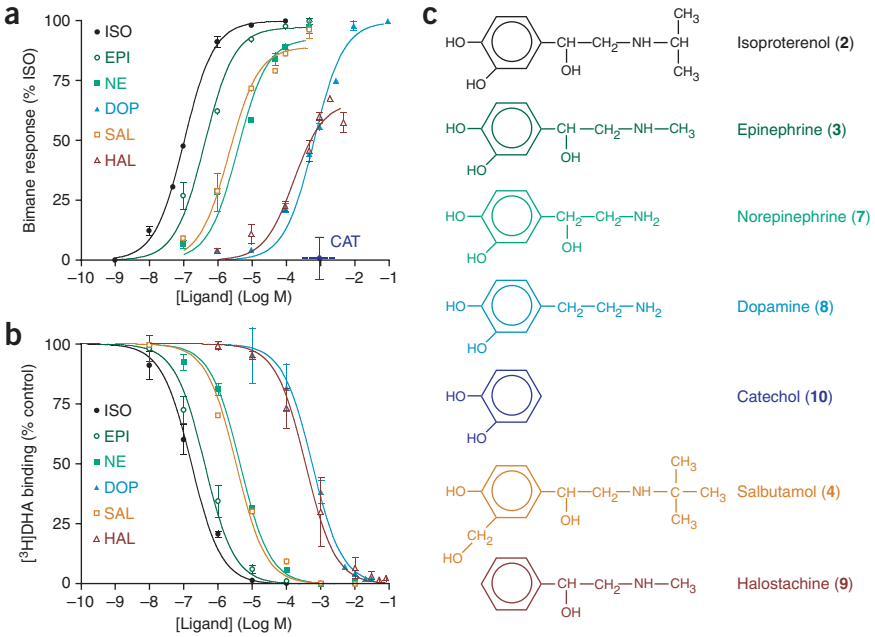

Figure 3 Bimane response to catechol and noncatechol agonists. (**a**) Dose-dependent bimane response of bimane-labeled β_2-AR–Δ5-Cys271+Trp135 for the catecholamine agonists isoproterenol (black, filled circle), epinephrine (dark green, outlined circle), norepinephrine (dark cyan, filled square), and dopamine (blue, filled triangle) and for the noncatechol partial agonists salbutamol (orange, outlined square) and halostachine (red, outlined triangle). The chart also shows the absence of response to a saturating dose of catechol (1 mM, purple diamond, dotted line). The response is expressed as the percentage of the reponse to a saturating dose of isoproterenol. Data are presented as the mean ± s.e.m. from three to seven independent experiments. (**b**) Binding of bimane-labeled β_2-AR–Δ5-Cys271+Trp135 to isoproterenol, epinephrine, norepinephrine, dopamine, salbutamol and halsotachine measured in competition with the radioligand [^{3}H]DHA. The results are expressed as percentage of bound radioligand in the absence of competitor and presented as the mean ± s.e.m. of three independent experiments performed in triplicate. (**c**) Chemical structure of the ligands used for the experiments in **a** and **b**.

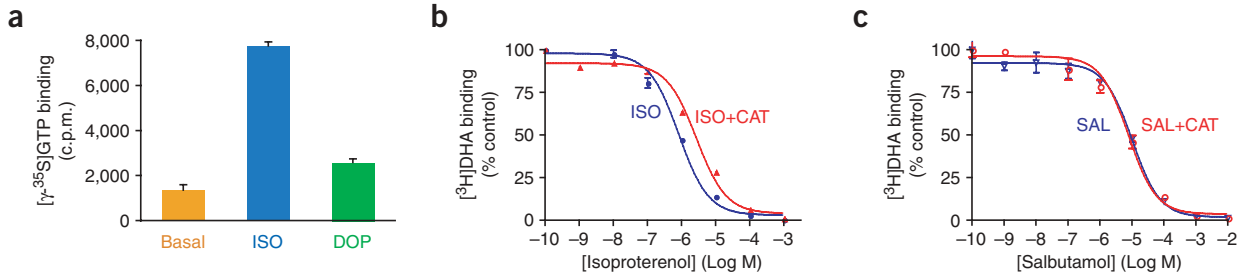

Figure 4 Functional interactions of β_2-AR–Δ5-Cys271+Trp135 with dopamine and catechol. (**a**) Dopamine and isoproterenol stimulated binding of [γ-^{35}S]GTP to purified G_s reconstituted with purified bimane-labeled β_2-AR–Δ5-Cys271+Trp135. The data are representative of two independent experiments performed in triplicate, shown as mean ± s.e.m. (**b**,**c**) Competition binding analysis on purified bimane-labeled β_2-AR–Δ5-Cys271+Trp135 reconstituted into phospholipid vesicles. We performed competition binding studies using 1 nM [^{3}H]DHA together with the indicated concentrations of isoproterenol (**b**) or salbutamol (**c**) in the absence or presence of 10 mM catechol. Catechol competes with isoproterenol (**b**), but not with salbutamol (**c**), for binding to bimane-labeled β_2-AR–Δ5-Cys271+Trp135. Binding experiments represent the average of three independent experiments performed in triplicate and are shown as mean ± s.e.m.

catechol may be a weak agonist that triggers the rotamer toggle switch in TM6 but does not disrupt the ionic lock between TM3 and TM6. This proposal is consistent with the recent two-dimensional crystal structure of metarhodopsin I (meta-I). Aligning the electron density map of meta-I with the three-dimensional structure of inactive rhodopsin reveals no detectable rigid body movements or rotations of helices[11]. Thus, in meta-I the ionic lock is still intact; yet there is evidence for a rearrangement around Trp265$^{6.48}$, adjacent to the retinal binding pocket. This rearrangement may involve changes in the rotameric position of Trp265$^{6.48}$ as well as a local distortion of the polypeptide backbone around Pro267$^{6.50}$ in TM6[11]. Thus, in both rhodopsin and the β_2-AR, conformational changes close to the ligand binding pocket are not rigidly coupled to structural modifications around the ionic lock. However, it should be noted that we have not been able to detect catechol-stimulated [γ-^{35}S]GTP binding in bimane-labeled β_2-AR–Δ5-Cys271+Trp135 reconstituted with Gs. Though this is likely due to the poor coupling efficiency of this modified receptor, we cannot exclude the possibility that the modifications made to β_2-AR to monitor the ionic lock altered the conformational response to catechol.

The agonist-induced change in bimane fluorescence in β_2-AR–Δ5-Cys271+Trp135 occurs with a $t_{1/2}$ of approximately 30 s in receptors reconstituted into phospholipid vesicles (data not shown). This is considerably slower than conformational changes observed in a modified α_2-AR containing a fluorescein arsenical hairpin (FlAsH) binder site in the third intracellular loop and having cyan fluorescent protein (CFP) fused to the carboxyl terminus[12,13]. This modified receptor was expressed in HEK293 human embryonic kidney cells and conformational changes were detected as changes in fluorescence resonance energy transfer (FRET) between FlAsH and CFP. There are several possible explanations for the observed differences in kinetics. The use of a large fluorescence reporter such as CFP does not allow one to determine the nature of the structural change that is responsible for the change in FRET; therefore, these FRET experiments may have been detecting a different conformational switch. Our previous studies provide evidence that agonist binding and activation occurs through a sequence of conformational changes having different rates[6,7]. However, the different rates observed could also be attributed to the fact that here we have studied purified receptors in the absence of G protein, whereas the FRET experiments were performed on receptors expressed in cell membranes that contained G proteins. Receptors form complexes with G proteins in the plasma membrane (an event called precoupling), and these complexes have a higher affinity for agonists than do receptors alone. Other factors that might contribute to differences between the results of our experiments using purified receptors and those of our experiments using receptors in cells could include the influence of the pH and salt gradients across the plasma membrane in living cells and the asymmetry of plasma membrane lipids. Finally, it is possible that the fluorescence changes we have observed reflect a conformational change that occurs following the disruption of the ionic lock and at a slower rate.

Table 1 Summary of the effect of different ligands on two molecular switches in the β_2-AR

Ligand	Efficacy	Rotamer toggle switch	Ionic lock
Isoproterenol	Full agonist	+	+
Epinephrine	Full agonist	+	+
Norepinephrine	Strong partial agonist	+	+
Salbutamol	Partial agonist	–	+
Dopamine	Weak partial agonist	+	+
Halostachine	Very weak partial agonist	–	+/–
Catechol	Very weak partial agonist	+	–
Alprenolol	Neutral antagonist	–	–
ICI-118,551	Inverse agonist	–	–

The structural basis of agonist efficacy in GPCRs is poorly understood. Using the evidence presented here and in recently published manuscripts[6,7], we propose a model in which agonists stabilize partially or fully active states by using different chemical groups to activate different combinations of molecular switches that are not necessarily interdependent. In the unliganded, inactive state of a GPCR, the arrangement of transmembrane segments is stabilized by noncovalent interactions among side chains. Structurally distinct ligands are able to break different combinations of the basal state–stabilizing interactions either directly by binding to amino acids that are involved in these intramolecular interactions, or indirectly by stabilizing new intramolecular interactions. These ligand-specific conformational changes may be responsible for differential activation of the signaling cascades of the receptor. The affinity of a particular ligand is then dependent on the energy costs and gains associated with each disrupted and created interaction, whereas its efficacy is dependent on the ability to trigger the switches associated with activation. These molecular switches are normally activated by agonist

binding[10,14], but they are also revealed in constitutively active mutants, in which single point mutations in virtually any structural domain can lead to elevated basal activity[15].

Based on our previous work[7] and on studies presented here, we observe that structurally different agonists have different effects on the rotamer toggle switch and the ionic lock (**Table 1**). Dopamine represents the minimal structure required for activation of both the rotamer toggle switch and the ionic lock, yet dopamine is not a full agonist. Thus, additional switches must be triggered by interactions between β_2-AR and structural components on norepinephrine, epinephrine and isoproterenol that are lacking in dopamine. These structural components include the chiral β-OH group and the amine substituent (**Fig. 3c**). The switches activated by these interactions may be involved in G protein activation as well as in other proteic interactions such as arrestin recruitment. A full understanding of these molecular switches will have direct repercussions in drug design, allowing better control of drug efficacy and affinity.

METHODS

DNA constructs. The template used for site-directed mutagenesis was described previously[16]. Briefly, we epitope tagged the coding sequence of the human β_2-AR (i) at the amino terminus with the cleavable influenza-hemagglutinin signal sequence followed by the Flag epitope and (ii) at the carboxyl terminus with six histidines[17]. In addition, we mutated 5 out of the 13 native cysteines as follows: C77V, C265A, C327S, C378A and C406A[16]. We introduced the I135W and A271C mutations using the QuickChange technique (Stratagene), and then we cloned the mutated cDNAs into the pFastBac1 vector (Invitrogen). We confirmed all constructs by restriction enzyme analysis and DNA sequencing.

Buffers. Buffer A consisted of 100 mM NaCl, 20 mM HEPES, pH 7.5, 0.1% dodecyl maltoside (Anatrace); buffer B consisted of buffer A with 0.01% cholesterol hemisuccinate (Steraloids Inc.).

Expression in Sf9 cells and purification. We grew Sf9 insect cells at 27 °C in suspension cultures in ESF-921 cell culture medium (Expression Systems) supplemented with 0.05 mg ml^{-1} gentamicin. We generated recombinant baculoviruses using the Bac-to-Bac Baculovirus Expression System (Invitrogen). Each virus strain went through two rounds of amplifications before we used it for receptor expression. We infected cells using a 1:500 dilution of high-titer virus stock at a density of 5 millions ml^{-1}. After infection, we incubated the cells for 48 h and then harvested them by centrifugation at 5,000*g* for 10 min. We stored the cell pellets at –80 °C until use, and we solubilized and purified the receptors from these cell pellets as previously described[7]. We eluted the resulting preparation in buffer B.

Bimane labeling of purified receptors. We mixed purified receptors and mBBr (Invitrogen) at the same molarity in buffer A and incubated the mixture overnight on ice in the dark. We purified the fluorophore-labeled receptors by gel filtration on a desalting column equilibrated with buffer B immediately before use. We performed fluorescence spectroscopy experiments on a Spex FluoroMax-3 spectrofluorometer (Jobin Yvon Inc.) with photon-counting mode by using an excitation and emission bandpass of 4 nm; we performed all experiments at 25 °C. For emission scans, we set excitation at 370 nm and measured emission from 430 to 480 nm with an integration time of 0.5 s nm^{-1}. To determine the effect of ligands, we took the spectra after 15 min incubation with the drugs. We corrected fluorescence intensity for background fluorescence from buffer and ligands in all experiments. For anisotropy experiments, we set the excitation wavelength at 390 nm, and we recorded emission in both the parallel ($I_{parallel}$) and perpendicular ($I_{perpendicular}$) orientations at 460 nm. We calculated anisotropy (r) according to the following formula:

$$r = (I_{parallel} - I_{perpendicular})(I_{parallel} + 2 \times I_{perpendicular})^{-1}$$

To determine the Stern-Volmer constant for the bimane-tryptophan interaction, we measured the emission spectrum of unreacted mBBr in the presence of different concentrations of tryptophan. We plotted the ratio F_0/F (fluorescence in the absence of quencher divided by fluorescence in the presence of quencher) as a function of tryptophan concentration; we then determined the Stern-Volmer constant from the slope of the linear regression.

Cysteine reaction rate. To measure the efficiency of cysteine labeling, we used a technique based on the fluorescent properties of fluorescein 5-maleimide (FM). After reacting with a cysteine, the fluorescence intensity of the FM is increased about four-fold, allowing measurement of the FM reaction rate (and therefore of cysteine reactivity). To make this measurement, we initiated the labeling reaction by adding 1 nM of FM to 500 µl of 100 nM purified receptor in buffer A. We then monitored the fluorescence signal in the Fluoromax-3 spectrofluorometer using 490 and 520 nm for the excitation and emission wavelengths, respectively. Because the receptor is used in large excess, the change in fluorescence intensity as a function of time follows a monoexponential curve, having an apparent rate proportional to the receptor concentration and to the actual reaction rate of the cysteine. We determined rate constants for the labeling reactions by fitting the time traces to a monoexponential curve using the program Prism (GraphPad). We obtained the actual rate constant of the labeling reaction by dividing the apparent rate constant by the receptor concentration.

Radioligand binding. We purchased the radioligand [^{3}H]dihydroalprenolol (DHA) from Amersham. For the pharmacological characterization, we prepared membrane proteins as described previously[17], and we determined the protein concentration by the method of Bradford using a commercial kit (DC protein assay, Bio-Rad). For binding on the purified, labeled receptor, we first reconstituted the receptors in phospholipid vesicles as described previously[7]. We carried out saturation binding and competition binding experiments as described previously[7,17]. We obtained all data points in triplicate and repeated experiments three or four times. We analyzed binding data by nonlinear regression analysis using Prism and we fitted this data with a hyperbolic function. We determined B_{max} and K_d values for [^{3}H]DHA in the membranes as the mean ± s.e. of $n = 3$–4. We calculated the K_i values of isoproterenol from the equation $K_i = IC_{50} \times (1 + [L]/K_d)^{-1}$, in which [L] is the [^{3}H]DHA concentration; we used the IC_{50} values for inhibition of [^{3}H]DHA binding by isoproterenol.

Molecular modeling. The residues of β_2-AR are numbered according to their position in the sequence followed by the Ballesteros general number[18] in superscript. In this nomenclature, each residue is identified by two numbers: the first (1 through 7) corresponds to the helix in which it is located; the second indicates its position relative to the most conserved residue in the transmembrane segment, identified on a multiple sequence alignment of class A GPCRs and arbitrarily assigned to 50. For instance, Trp135$^{3.54}$ is the tryptophan residue in position 135 of the β_2-AR sequence, located in TM3 four residues after the highly conserved Arg131$^{3.50}$. This scheme applies to all class A GPCRs and allows easy comparison among residues in the seven transmembrane segments of different receptors. We built a three-dimensional model of the β_2-AR in the inactive state by homology modeling using the crystal structure of bovine rhodopsin (PDB ID code 1GZM[19]) as a template, as described[7]. Moreover, we built a model of the active state of the β_2-AR in which TM6 is bent away from TM3[4], occupying a different region of the conformational space induced by the Cys285$^{6.47}$/Pro288$^{6.50}$ motif[10]. We studied the relative orientations of the bimane fluorophore and its interactions with the receptor using molecular dynamics simulations (as described[7]) in which bimane was parameterized with the Antechamber program using the General Amber Force Field (GAFF)[20] and atomic charges derived using the restrained electrostatic potential (RESP) method on a potential calculated ab-initio with the HF/6-31G* basis set. We created the figures of the three-dimensional models using Molscript 2.1.2 (Avatar Software)[21] and Raster 3D 2.7 (Biomolecular Structure Center at the University of Washington)[22].

Note: Supplementary information is available on the Nature Chemical Biology website.

ACKNOWLEDGMENTS

This work was supported by grants from the US National Institutes of Health (Grant 5 RO1 NS28471 to B.K. and Grant R01 DA14896 to D.F.) and the Mather's Charitable Foundation (to B.K.).

COMPETING INTERESTS STATEMENT
The authors declare that they have no competing financial interests.

Published online at http://www.nature.com/naturechemicalbiology
Reprints and permissions information is available online at http://npg.nature.com/reprintsandpermissions/

1. Ballesteros, J.A. *et al*. Activation of the beta 2-adrenergic receptor involves disruption of an ionic lock between the cytoplasmic ends of transmembrane segments 3 and 6. *J. Biol. Chem.* **276**, 29171–29177 (2001).
2. Greasley, P.J., Fanelli, F., Rossier, O., Abuin, L. & Cotecchia, S. Mutagenesis and modelling of the alpha(1b)-adrenergic receptor highlight the role of the helix 3/helix 6 interface in receptor activation. *Mol. Pharmacol.* **61**, 1025–1032 (2002).
3. Shapiro, D.A., Kristiansen, K., Weiner, D.M., Kroeze, W.K. & Roth, B.L. Evidence for a model of agonist-induced activation of 5-hydroxytryptamine 2A serotonin receptors that involves the disruption of a strong ionic interaction between helices 3 and 6. *J. Biol. Chem.* **277**, 11441–11449 (2002).
4. Farrens, D.L., Altenbach, C., Yang, K., Hubbell, W.L. & Khorana, H.G. Requirement of rigid-body motion of transmembrane helices for light activation of rhodopsin. *Science* **274**, 768–770 (1996).
5. Ghanouni, P. *et al.* Functionally different agonists induce distinct conformations in the G protein coupling domain of the beta 2 adrenergic receptor. *J. Biol. Chem.* **276**, 24433–24436 (2001).
6. Swaminath, G. *et al.* Sequential binding of agonists to the beta2 adrenoceptor. Kinetic evidence for intermediate conformational states. *J. Biol. Chem.* **279**, 686–691 (2004).
7. Swaminath, G. *et al.* Probing the beta2 adrenoceptor binding site with catechol reveals differences in binding and activation by agonists and partial agonists. *J. Biol. Chem.* **280**, 22165–22171 (2005).
8. Mansoor, S.E., McHaourab, H.S. & Farrens, D.L. Mapping proximity within proteins using fluorescence spectroscopy. A study of T4 lysozyme showing that tryptophan residues quench bimane fluorescence. *Biochemistry* **41**, 2475–2484 (2002).
9. Green, S.A., Cole, G., Jacinto, M., Innis, M. & Liggett, S.B. A polymorphism of the human beta 2-adrenergic receptor within the fourth transmembrane domain alters ligand binding and functional properties of the receptor. *J. Biol. Chem.* **268**, 23116–23121 (1993).
10. Shi, L. *et al.* Beta2 adrenergic receptor activation. Modulation of the proline kink in transmembrane 6 by a rotamer toggle switch. *J. Biol. Chem.* **277**, 40989–40996 (2002).
11. Ruprecht, J.J., Mielke, T., Vogel, R., Villa, C. & Schertler, G.F. Electron crystallography reveals the structure of metarhodopsin I. *EMBO J.* **23**, 3609–3620 (2004).
12. Hoffmann, C. *et al.* A FlAsH-based FRET approach to determine G protein-coupled receptor activation in living cells. *Nat. Methods* **2**, 171–176 (2005).
13. Vilardaga, J.P., Steinmeyer, R., Harms, G.S. & Lohse, M.J. Molecular basis of inverse agonism in a G protein-coupled receptor. *Nat. Chem. Biol.* **1**, 25–28 (2005).
14. Jongejan, A. *et al.* Linking agonist binding to histamine H1 receptor activation. *Nat. Chem. Biol.* **1**, 98–103 (2005).
15. Parnot, C., Miserey-Lenkei, S., Bardin, S., Corvol, P. & Clauser, E. Lessons from constitutively active mutants of G protein-coupled receptors. *Trends Endocrinol. Metab.* **13**, 336–343 (2002).
16. Gether, U. *et al.* Agonists induce conformational changes in transmembrane domains III and VI of the beta2 adrenoceptor. *EMBO J.* **16**, 6737–6747 (1997).
17. Kobilka, B.K. Amino and carboxyl terminal modifications to facilitate the production and purification of a G protein-coupled receptor. *Anal. Biochem.* **231**, 269–271 (1995).
18. Ballesteros, J. & Weinstein, H. Integrated methods for the construction of three-dimensional models and computational probing of structure-function relations in G protein-coupled receptors. *Methods Neurosci.* **25**, 366–428 (1995).
19. Li, J., Edwards, P.C., Burghammer, M., Villa, C. & Schertler, G.F. Structure of bovine rhodopsin in a trigonal crystal form. *J. Mol. Biol.* **343**, 1409–1438 (2004).
20. Wang, J., Wolf, R.M., Caldwell, J.W., Kollman, P.A. & Case, D.A. Development and testing of a general amber force field. *J. Comput. Chem.* **25**, 1157–1174 (2004).
21. Kraulis, P.J. MOLSCRIPT: a program to produce both detailed and schematic plots of protein structures. *J. Appl. Crystallogr.* **24**, 946–950 (1991).
22. Merritt, E.A. & Bacon, D.J. Raster3D: photorealistic molecular graphics. *Methods Enzymol.* **277**, 505–524 (1997).